Biochemical and Biophysical Research Communications 391 (2010) 762–767

Contents lists available at ScienceDirect

Biochemical and Biophysical Research Communications

journal homepage: www.elsevier.com/locate/ybbrc

Chromatin states of core pluripotency-associated genes in pluripotent, multipotent and differentiated cells

Sanna Barrand, Philippe Collas *

Institute of Basic Medical Sciences, Faculty of Medicine, University of Oslo, Oslo, Norway
Norwegian Center for Stem Cell Research, Oslo, Norway

ARTICLE INFO

Article history:
Received 17 November 2009
Available online 26 November 2009

Keywords:
Post-translational histone modification
DNA methylation
Pluripotency
Differentiation

ABSTRACT

Oct4, Nanog and Sox2 constitute a core of transcription factors controlling pluripotency. Differentiation and reprogramming studies have unraveled a few epigenetic modifications associated in relation to the expression state of *OCT4*, *NANOG* and *SOX2*. There is, however, no comprehensive map of chromatin states on these genes in human primary cells at different stages of differentiation. We report here a profile of DNA methylation and of 10 histone modifications on regulatory regions of *OCT4*, *NANOG* and *SOX2* in embryonal carcinoma cells, mesenchymal stem cells and fibroblasts. Bisulfite sequencing reveals correlation between promoter CpG methylation and repression of *OCT4*, but not *NANOG* or *SOX2*, suggesting distinct repression mechanisms. Whereas none of these genes, even when inactive, harbor repressive trimethylated H3K9, CpG hypomethylated *NANOG* and *SOX2*, but not CpG methylated *OCT4*, are enriched in repressive H3K27me3. H3K79me1 and H3K79me3 tend to parallel each other and are linked to repression. Moreover, we highlight an inverse relationship between H3K27me3 occupancy on promoters and H3K36me3 occupancy on coding regions of *OCT4*, *NANOG* and *SOX2*, suggesting a cross-talk between K27 and K36 methylation. Establishment of distinct repression mechanisms for pluripotency-associated genes may constitute a safeguard system to prevent promiscuous reactivation during development or differentiation.

Introduction

Maintenance of a pluripotent state in embryos and embryonic stem (ES) cells is conferred by a core of developmentally regulated transcription factors including the homeodomain proteins Oct4 and Nanog and the high-mobility group transcription factor Sox2 [1]. In ES cells, Oct4, Nanog and Sox2 bind to and regulate many common target genes, including themselves and one another [2,3]. Interaction between Oct4, Nanog and Sox2 has been proposed to constitute the core of a transcriptional regulatory network [2,3] important for controlling pluripotency and differentiation [4].

In addition to transcription factor binding, gene expression is also regulated by combinatorial modifications of DNA and chromatin. Cytosine methylation in CpG dinucleotides is a hallmark of long-term gene silencing by creating target sites for methyl-binding proteins which in turn recruit transcriptional repressors [5]. Notably, however, the effect of CpG methylation on transcription is dependent on CpG density in promoters [6], thus a stretch of methylated cytosines does not necessarily imply repression. Gene expression is also controlled by post-translational modifications (PTMs) on the N-terminal tail of histones, which modulate their interaction with DNA and the targeting of chromatin modifiers [7]. In particular, trimethylation of lysine 9 of histone H3 (H3K9me3) or H3K27me3 marks inactive genes, while active genes are enriched in H3K4me2, H3K4me3, acetylated H3K9 (H3K9ac) and H3K36me3. However, whereas in active genes H3K4me3 peaks over promoters and transcription start sites (TSSs), H3K36me3 preferentially occupies exons within gene bodies [8].

Differentiation of ES cells or embryonal carcinoma cells results in downregulation of *OCT4*, *NANOG* and *SOX2* expression, coinciding with partial and often mosaic DNA methylation, H3K9 deacetylation and H3K9 trimethylation on specific regulatory sequences [9–13]. Conversely, reprogramming of fibroblasts to a pluripotent state is accompanied by CpG demethylation on *OCT4* and *NANOG* promoters and acquisition of transcriptionally permissive histone PTMs [14,15]. These studies have provided valuable information on epigenetic regulation of these pluripotency-associated genes primarily in cell lines, however, they have collectively only as-

Abbreviations: ES cell, embryonic stem cell; ac, acetylated; me, methylated; PTM, post-translational modification; ChIP, chromatin immunoprecipitation; ASC, adipose mesenchymal stem cell; SF, skin fibroblast; TSS, transcription start site; RT-PCR, reverse transcriptase polymerase chain reaction; CR, coding region.

* Corresponding author. Address: University of Oslo, Institute of Basic Medical Sciences, Department of Biochemistry, PO Box 1112, Blindern, 0317 Oslo, Norway. Fax: +47 22851058.
E-mail address: philippe.collas@medisin.uio.no (P. Collas).

0006-291X/$ - see front matter © 2009 Elsevier Inc. All rights reserved.
doi:10.1016/j.bbrc.2009.11.134

sessed a limited number of PTMs associated genes in primary human cells.

We provide here a detailed profile of CpG methylation and of 10 histone PTMs on *OCT4*, *NANOG* and *SOX2* regulatory regions in pluripotent embryonal carcinoma cells, primary adipose mesenchymal stem cells (ASCs), primary dermal and epidermal skin fibroblasts (SFs) and primary keratinocytes. The results point to distinct and gene-dependent transcriptional repression mechanisms in multipotent and differentiated cells. These mechanisms involve methylation of DNA, H3K27 and H3K36, and deacetylation of H3K9.

Materials and methods

Cells. Human embryonal carcinoma NCCIT cells (American Type Culture Collection; www.atcc.org; cat# CRL-2073) were cultured as described [16]. $CD45^{-}CD31^{-}$ ASCs were purified from liposuction material from three donors and cultured as described [17]. Cultures from three donors were pooled to eliminate potential donor variation. Adult human epidermal keratinocytes were from Cascade Biologics (www.cascadebio.com; cat# C-005-5C), human dermal fibroblasts from Cell Applications (www.cellapplications.com; cat# 106-05a) and epidermal fibroblasts from American Type Culture Collection (cat# CRL-7449).

Antibodies. Antibodies against H3K4me2 (cat# ab7766-100) and H3K4me3 (cat# ab8580-100) were from Abcam (www.abcam.com). Antibodies to H3K9ac (cat# 06-942), H3K9me3 (cat# 07-442) , H3K27me3 (cat# 06-449) and H3K36me2 (cat# 07-369) were from Upstate (www.upstate.com), and antibodies to H3K9me1 (cat# CS-065-100), H3K36me1 (cat# pAb-089-050), H3K36me3 (cat# PAb-058-50), H3K79me1 (cat# CS-082-100) and H3K79me3 (cat# pAb-068-050) were from Diagenode (www.diagenode.com).

Bisulfite sequencing. DNA was purified by phenolchloroform isoamyalcohol extraction and bisulfite conversion performed using the MethylEasy DNA Bisulfite Modification kit (Human Genetic Signatures; www.geneticsignatures.com). Converted DNA was amplified using PCR primers listed in Supplementary Table 1 (see Fig. 1). PCR conditions were 95 °C for 7 min and 40 cycles of 95 °C for 1 min, 50/55/58/62 °C for 1 min (Supplementary Table 1) and 72 °C for 1 min, followed by 10 min at 72 °C. PCR products were eluted, cloned into bacteria and sequenced.

Chromatin immunoprecipitation (ChIP). ChIP was performed in at least two replicates as described [12]. In short, Dynabeads® Protein A (Invitrogen; www.invitrogen.com) were added to 90 µl RIPA buffer containing 2.4 µg primary antibody (or 7 µl for H3K9me1 and H3K79me1 antibodies) and incubated on a rotator at 4 °C. DNA and protein were cross-linked with 1% formaldehyde for 8 min at 1–2 × 10^6 cells per ml and cross-linking stopped with 125 mM glycine. Cross-linked cells were lysed in presence of 1% SDS and the lysate sonicated in 200 µl batches each for 8 × 30 s (NCCIT, SF and Ker) or 14 × 30 s (ASC) to produce chromatin fragments averaging ~400 bp. Insoluble debris were sedimented, the supernatant (chromatin) diluted to 0.5 A_{260} units in RIPA buffer, and incubated with antibody–bead complexes for 2 h at 4 °C. Pellets were washed in RIPA and TE, ChIP DNA was eluted and DNA isolated by phenol–chloroform–isoamylalcohol extraction. ChIP DNA was analyzed by real time PCR using IQ SYBR® Green (BioRad; www.biorad.com) with ChIP primers listed in Supplementary Table 1 (Fig. 1). PCR conditions were 95 °C for 3 min and 40 cycles of 95 °C for 30 s, 60 °C for 30 s and 72 °C for 30 s.

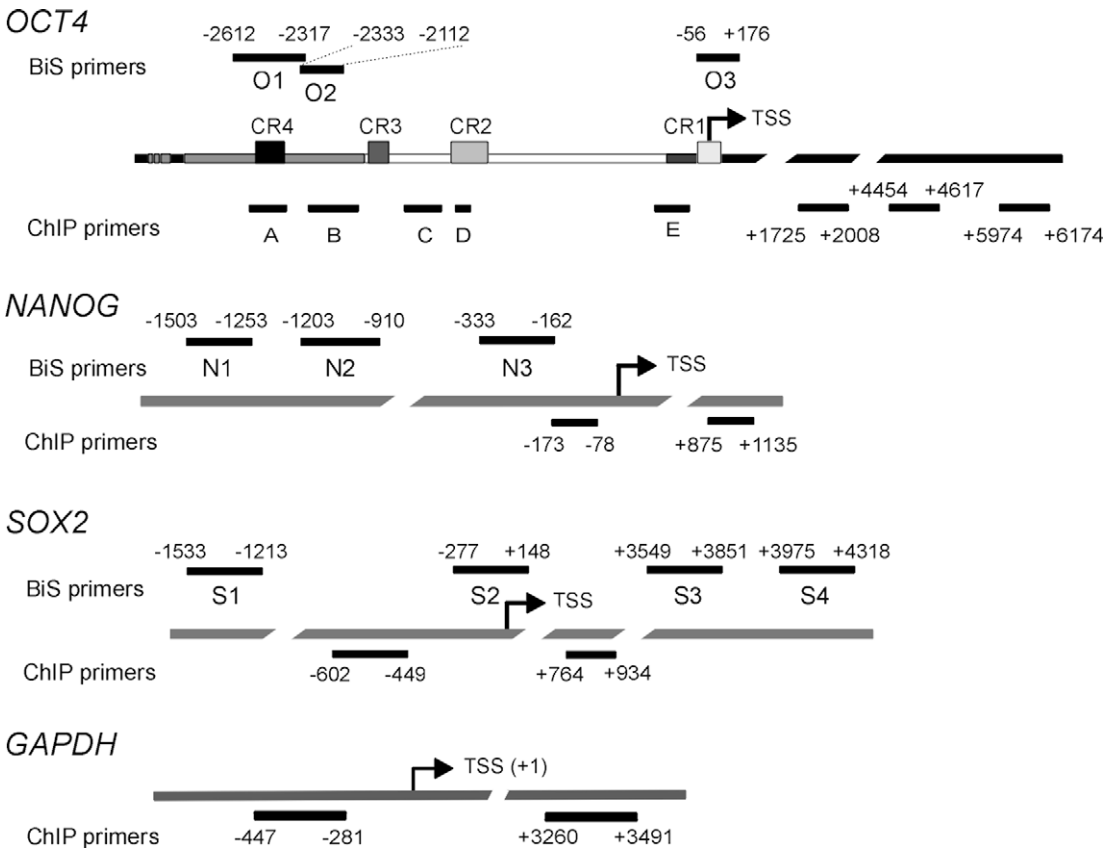

Fig. 1. Gene regulatory regions examined by ChIP and bisulfite sequencing (BiS). Position of each amplicon relative to the TSS (+1) is shown (see Supplementary Table 1 for details).

Reverse transcription (RT)-PCR. RT-PCR was carried from 0.5 μg total RNA using the Iscript cDNA synthesis kit (BioRad). cDNA (20 μl) was diluted 1:10 and 5 μl were used in PCR reactions using primers listed in Supplementary Table 2. PCR conditions were 95 °C for 3 min and 30 cycles of 95 °C for 30 s, 60 °C for 30 s and 72 °C for 30 s.

Results and discussion

Differential CpG methylation states of OCT4, NANOG and SOX2 in multipotent and differentiated cells suggest distinct transcriptional repression mechanisms

Long-term repression of transcription in general attributed to CpG methylation argues that the *OCT4*, *NANOG* and *SOX2* promoters would be DNA methylated in non-pluripotent cells, which do not express these genes. To test this hypothesis, we first confirmed by RT-PCR that *OCT4*, *NANOG* and *SOX2* were expressed in NCCIT embryonal carcinoma cells but not in ASCs, dermal SFs (Fig. 2A), epidermal SFs or keratinocytes (data not shown). We then analyzed by bisulfite sequencing the methylation state of 19 CpGs in the *OCT4* promoter, 14 CpGs in the *NANOG* promoter, and 35 CpGs in the *SOX2* promoter together with 12 CpGs in the *SOX2* regulatory region within positions +3549/+4318 downstream of TSS [11] (Fig. 1). Of note, our bisulfite sequencing and ChIP assays (see below) did not discriminate between *OCT4A* and the recently identified ES cell-specific *OCT4B1* isoforms [18]; however, this was likely of little significance here because these differ in their N-termini, arguing that they are transcribed from the same promoter.

In NCCIT cells all promoters were unmethylated, in agreement with gene expression (Fig. 2B). In ASCs, *OCT4* was hypermethylated relative to NCCIT ($P < 0.001$), consistent with its repression in this cell type, whereas *NANOG* and *SOX2* were largely unmethylated despite transcriptional inactivity (Fig. 2B). We nevertheless noted frequent methylation of three CpGs closer to the TSS of *NANOG*, however, spreading of these CpGs over the width of the region sequenced (167 bp) may be argued to constitute a globally weak methylation state. These profiles were similar in bone marrow mesenchymal stem cells (data not shown). Fibroblasts displayed similar methylation patterns to ASCs, with mosaic *OCT4* methylation and virtually no *NANOG* or *SOX2* methylation despite the repressed state of these genes (Fig. 2B), and similar methylation patterns were observed in primary keratinocytes (Fig. 2B). Thus, mosaic methylation of *OCT4* and no or poor methylation of *NANOG* and *SOX2* are features of multipotent and of differentiated cells. Moreover, whereas *OCT4* promoter methylation correlates with transcriptional inactivity, the methylation state of *NANOG* and *SOX2* cannot account for their repressed state, arguing for other repressive mechanisms for these genes. Interestingly, the hypomethylated state of *NANOG* and *SOX2* may constitute a permissive state enabling reactivation of the genes upon nuclear reprogramming to pluripotency [14].

Of note, differential methylation of the N3 region in the *NANOG* promoter (closest to the TSS) observed in our study is consistent with its inclusion in a putative tissue-dependent and differentially methylated region extending up to 1 kb upstream of the TSS, such as that proposed for mouse *Nanog* [13]. The significance of these methylation changes, though, remains uncertain as RT-PCR data

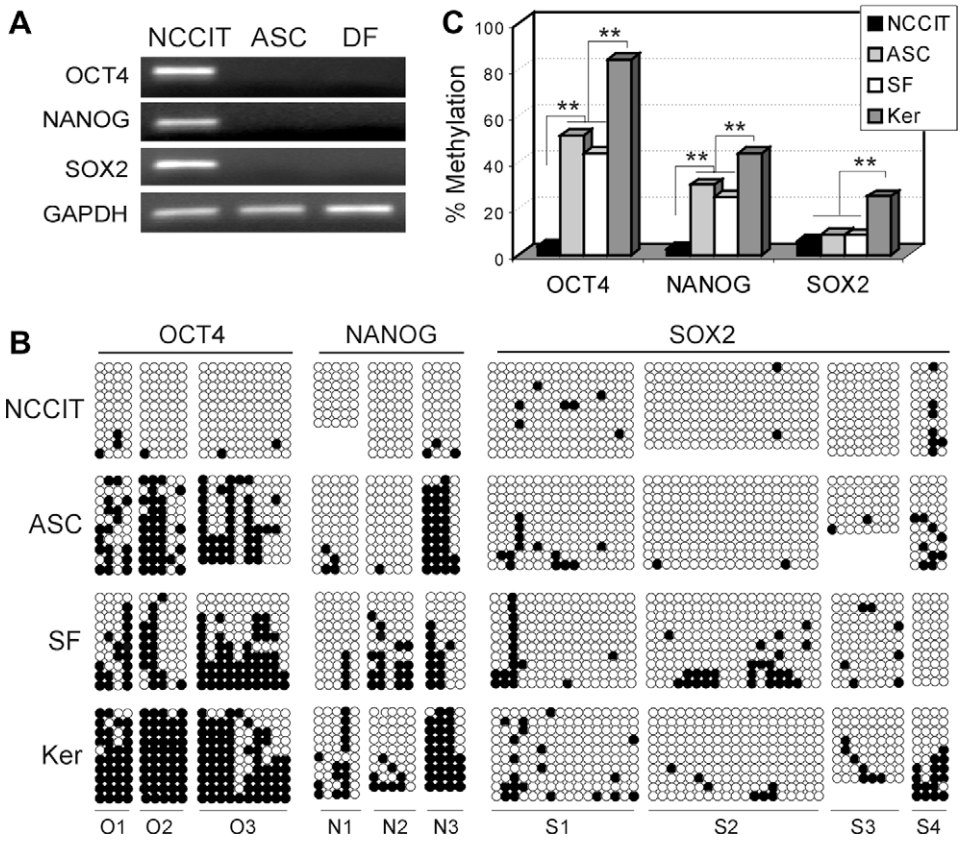

Fig. 2. Differential CpG methylation states of *OCT4*, *NANOG* and *SOX2* suggest distinct transcription repression mechanisms. (A) RT-PCR analysis of *OCT4*, *NANOG* and *SOX2* expression in NCCIT cells, ASCs and fibroblasts. (B) Bisulfite sequencing analysis of CpG methylation on *OCT4*, *NANOG* and *SOX2* regulatory regions in indicated cell types. Each CpG is represented by a circle in the 5′–3′ orientation; each row represents the methylation state deducted from the sequence of one bacterial clone of PCR product. O1–O3, N1–N3 and S1–S4 refer to amplicons shown in Fig. 1. ○, unmethylated CpG; ●, methylated CpG. (C) Percentage of CpG methylation for each genomic region in indicated cell types (**$P < 0.001$ between cell types; χ^2-test).

do not enable a correlation between *NANOG* methylation and expression in the cell types studied. Differentiation of ES cells and conversely, reprogramming of fibroblasts to ES-like cells are accompanied by changes in *NANOG* methylation in the differentially methylated region [14,19]; nevertheless methylation may not constitute a primary mechanism of repression *per se* but may be established following repression by other mechanisms. The lack of reactivation of *NANOG*, but not *OCT4*, after treatment of mouse cells with the DNA methyltransferase inhibitor 5-azacytidine and the histone deacetylase inhibitor trichostatin A [13,20], supports this view.

Differential enrichment of OCT4, NANOG and SOX2 promoters in repressive histone modifications

As DNA methylation could not account for *NANOG* or *SOX2* repression in the cells examined, we next examined by ChIP how histone PTMs would correlate with transcription states of *OCT4*, *NANOG* and *SOX2*. We first showed that the housekeeping *GAPDH* gene promoter was occupied by permissive H3K4me2, H3K4me3 and H3K9ac and devoid of repressive H3K9me3 and H3K27me3 in all cell types (Fig. 3A and B). A similar enrichment pattern was observed on the active *OCT4*, *SOX2* and *NANOG* promoters in NCCIT cells. In contrast, the repressed state of these genes in ASCs and fibroblasts was reflected by the absence of K9 acetylation and, on *NANOG* and *SOX2*, enrichment in H3K27me3 (Fig. 3A). *OCT4*, however, showed virtually no H3K27me3 throughout the region examined (Fig. 3A; Supplementary Fig. 1A). Moreover, we observed high levels of di- and tri-methylated H3K4 on all promoters regardless of cell type and expression, consistent with the genome-wide observation that H3K4me3 is associated with the majority of promoters regardless of expression [21]. However, no H3K9me3 was detected on any promoter examined despite their inactive state, in contrast to H3K9me1 which occupied *OCT4*, *SOX2* and *NANOG* (but not *GAPDH*) predominantly in ASCs and fibroblasts (Fig. 3A). Thus H3K9me1 appears to be associated with repressed promoters in the absence of H3K9me3 in a manner compatible with H3K27me3 occupancy. Collectively, our results argue that trimethylation of H3K27, but not K9, contributes to the repressed state of *NANOG* and *SOX2* in ASCs and fibroblasts. *OCT4* harbors essentially neither H3K27me3 nor H3K9me3 but is CpG methylated, suggesting that it is repressed by DNA methylation. H3K9me1 may also have a repressive function on *OCT4*, *NANOG* and *SOX2*.

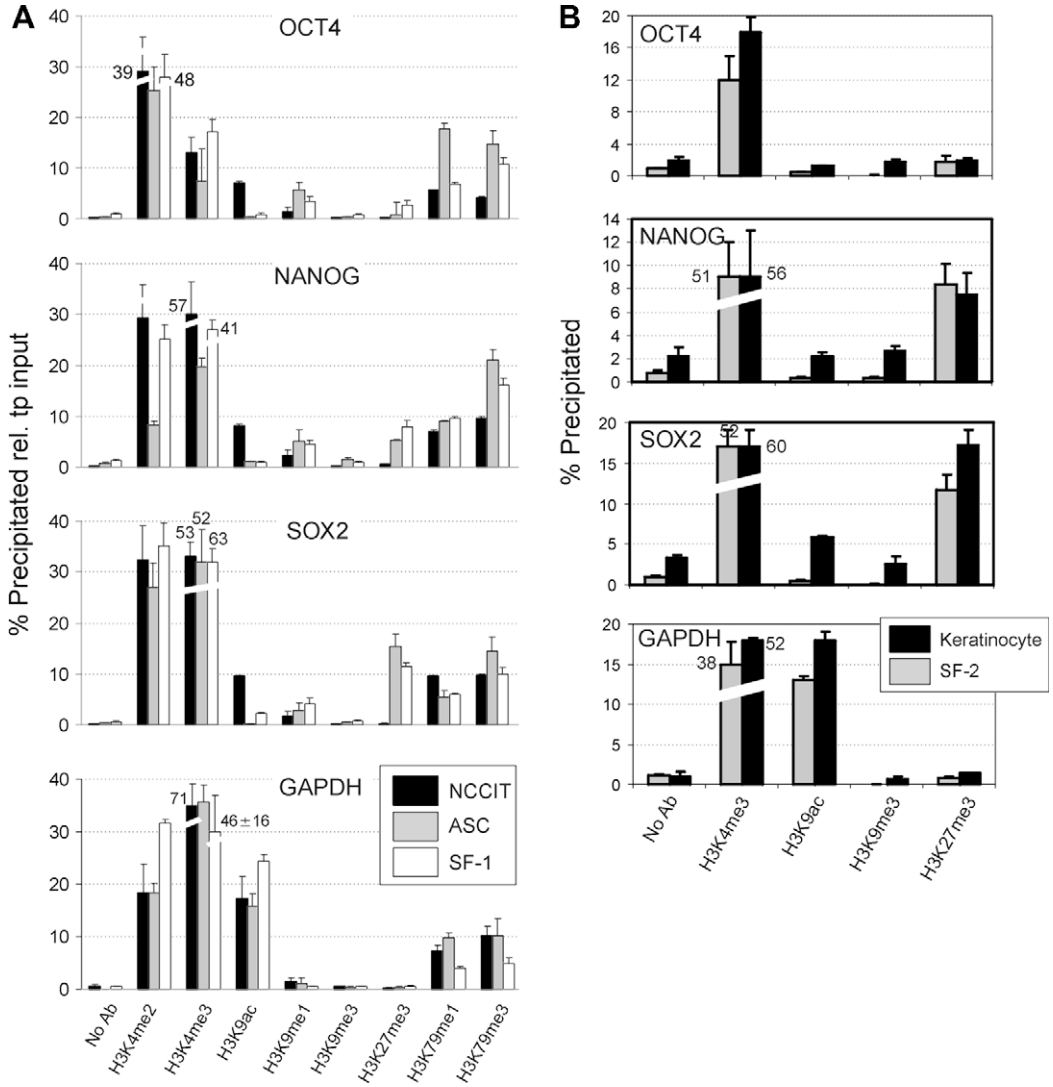

Fig. 3. Histone modification profiles in the regulatory regions of *OCT4*, *NANOG*, *SOX2* and *GAPDH*. (A) ChIP analysis of indicated H3 modifications in (A) NCCIT cells, ASCs and dermal fibroblasts and (B) keratinocytes and epidermal fibroblasts. Data are expressed as percent precipitated relative to input DNA (mean ± SD of at least two ChIPs each analyzed by duplicate qPCR).

To determine whether differential enrichment of H3K27me3 on *OCT4* and *NANOG* or *SOX2* was specific for ASCs and fibroblasts, we examined a different primary fibroblast (epidermal) culture and keratinocytes. In both cell types, *OCT4* did not exhibit any H3K27me3 (Fig. 3B; Supplementary Fig. 1B) in contrast to *NANOG* and *SOX2*, despite their repressed state (data not shown). H3K9me3 was again not detected, suggesting that it plays no significant role in repressing these genes in these cell types either (Fig. 3B). Notably as in ASCs or fibroblasts, H3K27me3 was anti-correlated with CpG methylation, reinforcing our finding that DNA methylation and H3K27 trimethylation are mutually exclusive on these promoters. These results collectively suggest that expression of *OCT4* is differently regulated from that of *NANOG* or *SOX2*.

Next, we showed that mono- and tri-methylated H3K79 were enriched on all promoters in all cell types, indicating occupancy independent of promoter activity (Fig. 3A). However, we detected more H3K79me3 on the *OCT4* and *NANOG* promoters in ASCs and fibroblasts than in NCCIT, suggesting a correlation between extent of H3K79 trimethylation and transcriptional inactivity. Moreover, the similar enrichment level on the *SOX2* promoter in all cell types may be linked to the high CpG content of the *SOX2* locus, but this remains to be investigated.

Overall, with the exception of *NANOG*, levels of H3K79me1 and H3K79me3 paralleled each other such that it was difficult to attribute a specific function to mono- or tri-methylated H3K79. In support of this view, Dot1-mediated H3K79 methylation has been shown to cause functional redundancy in the methylation states of H3K79, *a priori* limiting the function of specific H3K79 methylation states [22]. Nonetheless, our data indicate that H3K79 mono- and/or tri-methylation correlates with silencing of at least non-CpG island promoters (*OCT4* and *NANOG*). An implication of H3K79 methylation in transcriptional repression remains to be shown but would be consistent with recent evidence for its involvement in telomeric silencing [22].

Inverse relationship between H3K27me3 occupancy on promoters and H3K36me3 occupancy on coding regions

Trimethylation of H3 on K36 has been considered as a marker of transcriptional elongation because it is co-enriched with the Ser2-phosphorylated elongating form of RNA polymerase (Pol) II on the coding region (CR) of expressed genes [23]. We thus investigated how methylation of H3K36 correlated with transcription states of *OCT4*, *NANOG* and *SOX2*. In NCCIT, H3K36me3 was essentially undetected on promoters but enriched in the CRs (Fig. 4A and B). This pattern was consistent with H3K36me3 as a mark of elongation [24]. H3K36me3 was also at background level on the *NANOG* and *SOX2* promoters in ASCs and dermal fibroblasts, but occupied *OCT4*, at least in ASCs, at low levels (Fig. 4A). This pattern was confirmed by more extensive analysis of the *OCT4* promoter, particularly in ASCs and notably, levels of H3K36me3 on *OCT4* in ASCs increased more proximally to the TSS and reached a maximum in the CR (Fig. 4B). H3K36me3 was also detected in the CR of *GAPDH* and unexpectedly of *OCT4* in ASCs and dermal fibroblasts, and thus seemingly independently of expression (Fig. 4A). However, extension of PCR cycles by real time analysis showed low yet detectable levels of *OCT4* transcripts in ASCs and SFs (data not shown), which would be compatible with occupancy of H3K36me3 on the *OCT4* CR in these cells. Lastly, H3K36me3 was only weakly detected on the CRs of *NANOG* and *SOX2*, in agreement with the inactive state of these genes in these cells.

We found less consistent occupancy profiles for H3K36me1 on promoters and CRs as a function of expression or H3K27me3 enrichment (Fig. 4A). Nonetheless, we detected H3K36me1 on the *OCT4* promoter, which paralleled H3K36me3 occupancy and correlated with the absence of H3K27me3. Lastly, we did not detect any occupancy by H3K36me2 irrespective of levels of the mono- and tri-methylated forms (Fig. 4A). Unlike H3K36me3, recovery of mono- and di-methylated H3K36 from CRs has been shown not to correlate with transcriptional activity [24], and is independent of the presence of the H3K36 trimethylase HYPB/SetD2 [24].

Altogether, these results indicate that mono- and tri-methylated H3K36 occupancy on the *OCT4* promoter correlates with occupancy by K9me1, K79me1 and K79me3. However, absence of H3K36me3 on promoters of *NANOG* and *SOX2* correlates with occupancy by H3K27me3, which is in turn undetectable on *OCT4*. In addition, promoter occupancy by H3K27me3 correlates with no H3K36me3 on CRs, and conversely, absence of promoter H3K27me3 coincides with high H3K36me3 levels on CRs. This

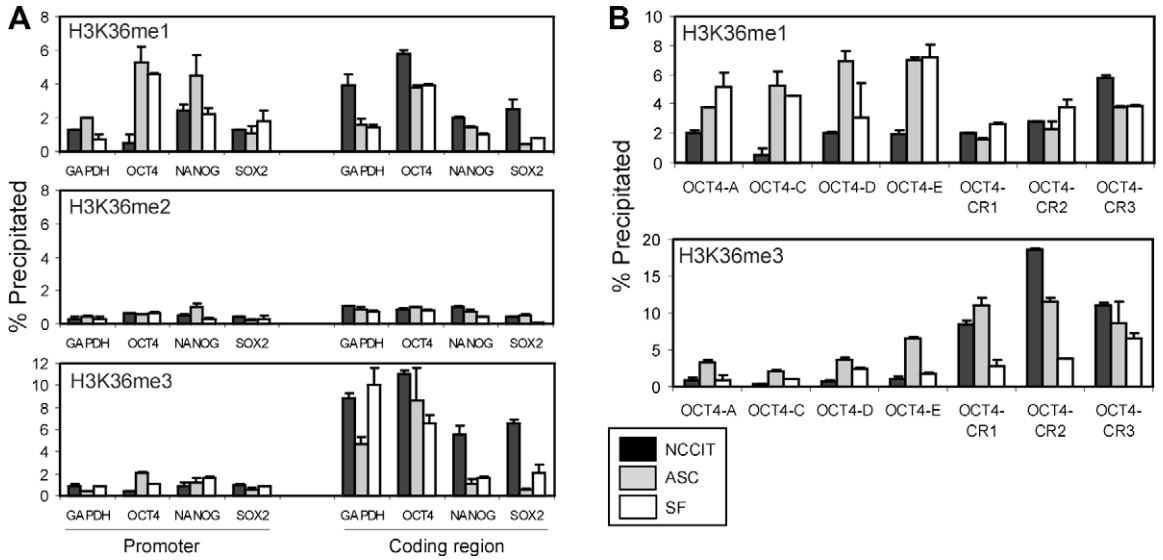

Fig. 4. Differential enrichment of mono- and tri-methylated H3K36 on promoters and coding regions in undifferentiated and differentiated cells. (A) ChIP analysis of H3K36me1, H3K36me2 and H3K36me3 on promoter (P) and coding regions (CR) of *GAPDH*, *OCT4*, *NANOG* and *SOX2*. (B) ChIP analysis of H3K36me1 and H3K26me3 on the *OCT4* promoter (amplicons OCT4A-E) and CR (OCT4-CR1-3; see Fig. 1).

highlights an inverse relationship between promoter enrichment in H3K27me3 and H3K36me3 occupancy on the gene body.

H3K36m3 enrichment in the immediate vicinity of the TSS and in CRs may constitute a mechanism to inhibit transcription initiation from cryptic sites in exons. Interestingly, a resent report suggests a link between trimethylation of exon H3K36 and promoter H3K27 [25]. Indeed, a knock-down of HYPB/SetD2 diminished levels of H3K36me3 and elevated levels of H3K27me3 in the 3′ end and 5′ end, respectively, of the *PABPCI* gene [25]. Thus, a hypothesis to be tested is that low levels of H3K27me3 on the *OCT4* promoter in ASCs and fibroblasts are coupled to H3K36me3 enrichment on both promoter and exon. In this respect, it will be interesting to investigate the distribution of the H3K27 histone methyltransferase Ezh2 and of the H3K36 methyltransferase HYPB/SetD2 throughout the *OCT4*, *NANOG* and *SOX2* loci as a function of their expression state.

How H3K36 and H3K27 trimethylation functionally inversely relate to one another may also involve demethylation activity on K27. Interestingly, the finding that the H3K27me3 demethylase UTX progresses along chromatin together with the RNA Poll II complex [26] suggests that SetD2 or a SetD2-associated factor may be involved in recruiting an H3K27me3 demethylase on chromatin [27]. This hypothesis may not only yield gene bodies but also promoter regions. Indeed, we show here that among the developmentally regulated genes examined, the *OCT4* promoter, which harbors essentially no H3K27me3, is the only one enriched in H3K36me3 on the coding region. The interplay between methylation on H3K36 and K27 on chromatin and transcription states remains to be examined closely.

In summary, we provide a detailed chromatin state map of *OCT4*, *NANOG* and *SOX2* regulatory regions and indications on the differential mechanism of transcriptional repression of these genes in MSCs and differentiated cells. Establishment of distinct repression mechanisms for pluripotency-associated genes may constitute a safeguard system to prevent promiscuous activation of these genes during development or differentiation. Furthermore, understanding the nature of histone PTMs on regulatory regions of pluripotency-associated genes should constitute a platform for designing rationalized means of efficiently inducing pluripotency by manipulating epigenetic programs.

Acknowledgments

We thank Kristin Vekterud for technical assistance and Dr. Agate Noer for valuable advice. This work was supported by the Research Council of Norway and the Norwegian Center for Stem Cell Research.

Appendix A. Supplementary data

Supplementary data associated with this article can be found, in the online version, at doi:10.1016/j.bbrc.2009.11.134.

References

[1] I. Chambers, S.R. Tomlinson, The transcriptional foundation of pluripotency, Development 136 (2009) 2311–2322.
[2] L.A. Boyer, T.I. Lee, M.F. Cole, S.E. Johnstone, S.S. Levine, J.P. Zucker, M.G. Guenther, R.M. Kumar, H.L. Murray, R.G. Jenner, D.K. Gifford, D.A. Melton, R. Jaenisch, R.A. Young, Core transcriptional regulatory circuitry in human embryonic stem cells, Cell 122 (2005) 947–956.
[3] Y.H. Loh, Q. Wu, J.L. Chew, V.B. Vega, W. Zhang, X. Chen, G. Bourque, J. George, B. Leong, J. Liu, K.Y. Wong, K.W. Sung, C.W. Lee, X.D. Zhao, K.P. Chiu, L. Lipovich, V.A. Kuznetsov, P. Robson, L.W. Stanton, C.L. Wei, Y. Ruan, B. Lim, H.H. Ng, The Oct4 and Nanog transcription network regulates pluripotency in mouse embryonic stem cells, Nat. Genet. 38 (2006) 431–440.
[4] J. Silva, A. Smith, Capturing pluripotency, Cell 132 (2008) 532–536.
[5] R.J. Klose, A.P. Bird, Genomic DNA methylation: the mark and its mediators, Trends Biochem. Sci. 31 (2006) 89–97.
[6] M. Weber, I. Hellmann, M.B. Stadler, L. Ramos, S. Paabo, M. Rebhan, D. Schubeler, Distribution, silencing potential and evolutionary impact of promoter DNA methylation in the human genome, Nat. Genet. 39 (2007) 457–466.
[7] T. Kouzarides, Chromatin modifications and their function, Cell 128 (2007) 693–705.
[8] P. Kolasinska-Zwierz, T. Down, I. Latorre, T. Liu, X.S. Liu, J. Ahringer, Differential chromatin marking of introns and expressed exons by H3K36me3, Nat. Genet. 41 (2009) 376–381.
[9] P. Deb-Rinker, D. Ly, A. Jezierski, M. Sikorska, P.R. Walker, Sequential DNA methylation of the Nanog and Oct-4 upstream regions in human NT2 cells during neuronal differentiation, J. Biol. Chem. 280 (2005) 6257–6260.
[10] N. Feldman, A. Gerson, J. Fang, E. Li, Y. Zhang, Y. Shinkai, H. Cedar, Y. Bergman, G9a-mediated irreversible epigenetic inactivation of Oct-3/4 during early embryogenesis, Nat. Cell Biol. 8 (2006) 188–194.
[11] M. Sikorska, J.K. Sandhu, P. Deb-Rinker, A. Jezierski, J. Leblanc, C. Charlebois, M. Ribecco-Lutkiewicz, M. Bani-Yaghoub, P.R. Walker, Epigenetic modifications of SOX2 enhancers, SRR1 and SRR2, correlate with in vitro neural differentiation, J. Neurosci. Res. 86 (2008) 1680–1693.
[12] J.A. Dahl, P. Collas, Q^2ChIP, a quick and quantitative chromatin immunoprecipitation assay unravels epigenetic dynamics of developmentally regulated genes in human carcinoma cells, Stem Cells 25 (2007) 1037–1046.
[13] N. Hattori, Y. Imao, K. Nishino, N. Hattori, J. Ohgane, S. Yagi, S. Tanaka, K. Shiota, Epigenetic regulation of Nanog gene in embryonic stem and trophoblast stem cells, Genes Cells 12 (2007) 387–396.
[14] K. Takahashi, K. Tanabe, M. Ohnuki, M. Narita, T. Ichisaka, K. Tomoda, S. Yamanaka, Induction of pluripotent stem cells from adult human fibroblasts by defined factors, Cell 131 (2007) 861–872.
[15] N. Maherali, R. Sridharan, W. Xie, J. Utikal, S. Eminli, K. Arnold, M. Stadtfeld, R. Yachechko, J. Tchieu, R. Jaenisch, K. Plath, K. Hochedlinger, Directly reprogrammed fibroblasts show global epigenetic remodeling and widespread tissue contribution, Cell Stem Cell 1 (2007) 55–70.
[16] C.K. Taranger, A. Noer, A.L. Sorensen, A.M. Hakelien, A.C. Boquest, P. Collas, Induction of dedifferentiation, genome-wide transcriptional programming, and epigenetic reprogramming by extracts of carcinoma and embryonic stem cells, Mol. Biol. Cell 16 (2005) 5719–5735.
[17] A.C. Boquest, A. Shahdadfar, K. Fronsdal, O. Sigurjonsson, S.H. Tunheim, P. Collas, J.E. Brinchmann, Isolation and transcription profiling of purified uncultured human stromal stem cells: alteration of gene expression after in vitro cell culture, Mol. Biol. Cell 16 (2005) 1131–1141.
[18] Y. Atlasi, S.J. Mowla, S.A. Ziaee, P.J. Gokhale, P.W. Andrews, OCT4 spliced variants are differentially expressed in human pluripotent and nonpluripotent cells, Stem Cells 26 (2008) 3068–3074.
[19] S. Yeo, S. Jeong, J. Kim, J.S. Han, Y.M. Han, Y.K. Kang, Characterization of DNA methylation change in stem cell marker genes during differentiation of human embryonic stem cells, Biochem. Biophys. Res. Commun. 359 (2007) 536–542.
[20] N. Hattori, K. Nishino, Y.G. Ko, N. Hattori, J. Ohgane, S. Tanaka, K. Shiota, Epigenetic control of mouse Oct-4 gene expression in embryonic stem cells and trophoblast stem cells, J. Biol. Chem. 279 (2004) 17063–17069.
[21] T.S. Mikkelsen, M. Ku, D.B. Jaffe, B. Issac, E. Lieberman, G. Giannoukos, P. Alvarez, W. Brockman, T.K. Kim, R.P. Koche, W. Lee, E. Mendenhall, A. O'Donovan, A. Presser, C. Russ, X. Xie, A. Meissner, M. Wernig, R. Jaenisch, C. Nusbaum, E.S. Lander, B.E. Bernstein, Genome-wide maps of chromatin state in pluripotent and lineage-committed cells, Nature 448 (2007) 553–560.
[22] F. Frederiks, M. Tzouros, G. Oudgenoeg, T. van Welsem, M. Fornerod, J. Krijgsveld, F. van Leeuwen, Nonprocessive methylation by Dot1 leads to functional redundancy of histone H3K79 methylation states, Nat. Struct. Mol. Biol. 15 (2008) 550–557.
[23] B. Li, L. Howe, S. Anderson, J.R. Yates III, J.L. Workman, The Set2 histone methyltransferase functions through the phosphorylated carboxyl-terminal domain of RNA polymerase II, J. Biol. Chem. 278 (2003) 8897–8903.
[24] J.W. Edmunds, L.C. Mahadevan, A.L. Clayton, Dynamic histone H3 methylation during gene induction: HYPB/Setd2 mediates all H3K36 trimethylation, EMBO J. 27 (2008) 406–420.
[25] S.M. Yoh, J.S. Lucas, K.A. Jones, The Iws1:Spt6:CTD complex controls cotranscriptional mRNA biosynthesis and HYPB/Setd2-mediated histone H3K36 methylation, Genes Dev. 22 (2008) 3422–3434.
[26] E.R. Smith, M.G. Lee, B. Winter, N.M. Droz, J.C. Eissenberg, R. Shiekhattar, A. Shilatifard, *Drosophila* UTX is a histone H3 Lys27 demethylase that colocalizes with the elongating form of RNA polymerase II, Mol. Cell. Biol. 28 (2008) 1041–1046.
[27] T. Swigut, J. Wysocka, H3K27 demethylases, at long last, Cell 131 (2007) 29–32.